

Polarization-Reconfigurable Single-Port Patch Antenna with Switchable Horizontal and Vertical Modes for Mid-Band 5G Applications

Bhaben Saikia¹, Subasit Borah², and Kunal Borah³

¹Department of Electronics, Dhemaji College, Assam, India

²Department of Electronics and Communication Engineering, Indian Institute of Information Technology (IIIT) Manipur, India

³Department of Physics, North Eastern Regional Institute of Science and Technology (NERIST), Arunachal Pradesh, India

Corresponding author: Kunal Borah (e-mail: kbnerist@nerist.ac.in).

ABSTRACT With the growing demand for compact, high-performance and reconfigurable antenna systems in mid-band 5G communication (3.3–6 GHz), polarization agility has become essential for improving link reliability and spectral efficiency. This paper presents the design, simulation and experimental validation of a polarization reconfigurable microstrip patch antenna capable of dynamically switching between vertical (VP) and horizontal (HP) linear polarization states using a single RF excitation port. The antenna employs two orthogonal microstrip feedlines connected via PIN diode switches to a common feed, enabling selective excitation of adjacent patch edges. This facilitates activation of the fundamental TM₀₁ or TM₁₀ mode, producing vertical or horizontal polarization, respectively. Fabricated on an FR4 substrate, the antenna features a low-profile, planar configuration ideal for compact RF systems. Simulated and measured resonances occur at 5.31/5.40 GHz (VP) and 5.27/5.33 GHz (HP), respectively. The antenna achieves –10 dB impedance bandwidths of 3.52% (VP) and 6.01% (HP), peak gains of 2.48 dBi and 2.76 dBi and axial ratios above 48 dB, confirming high polarization purity and low cross-polarization. Radiation patterns show good agreement with simulations. The proposed design offers a compact and efficient solution for applications demanding polarization reconfigurability, making it well-suited for advanced wireless communication systems.

INDEX TERMS Microstrip patch antenna, polarization reconfigurable, mid-band 5G

I. INTRODUCTION

The exponential growth of wireless communication technologies has catalysed an ever-increasing demand for high-capacity, reliable and spectrum-efficient systems [1]. The evolution of modern wireless networks has led to the widespread development of multiple-band antennas [2-4]. These antennas are essential for heterogeneous applications where a single device must support multiple communication standards, such as GSM, 4G LTE, and various sub-6 GHz 5G bands. However, while multiband antennas offer frequency flexibility, they often struggle with signal degradation caused by multipath fading in complex urban environments.

To address these deleterious effects, polarization diversity has emerged as an effective and robust technique. By leveraging the orthogonal polarization states of electromagnetic waves—such as linear (horizontal or vertical) and circular polarizations—polarization diversity facilitates the reception of multiple, decorrelated signal copies, significantly reducing the probability of simultaneous fading across all polarizations [5]. This diversity mechanism not only enhances the reliability of wireless links but also supports frequency reuse, thereby

improving spectral efficiency—a key objective in congested and spectrum-scarce environments [6].

Over the past two decades, considerable research has focused on the design and optimization of polarization reconfigurable antennas (PRAs), which provide dynamic adaptability by switching between different polarization modes, providing the necessary diversity [7]. These reconfigurable systems offer greater flexibility and adaptability over conventional fixed-polarization antennas, enabling enhancements in capacity, interference mitigation and energy efficiency [8-9]. Among various antenna types explored for reconfigurable polarization functionalities, microstrip patch antennas and slot antennas have reaped particular attention due to their low-profile structure, ease of fabrication and compatibility with printed circuit board (PCB) technologies [10-12].

To achieve polarization reconfigurability, numerous mechanisms have been proposed, including the integration of radio-frequency (RF) switching elements such as PIN diodes, microelectromechanical systems (MEMS), varactors and photoconductive switches. Strategically embedded within the antenna geometry, these switches alter the surface current distribution upon activation, effectively

modifying the radiated polarization state [13–14]. However, a notable drawback of many existing PRAs is their reliance on multiple excitation ports, where each port typically excites a different polarization mode. While this approach can be effective, it inherently increases the complexity of the feeding network, demands additional RF circuitry and expands the antenna footprint—factors that hinder miniaturization and integration, particularly in compact wireless platforms [15–17].

Unlike conventional reconfigurable antennas that use dual ports or complex feeding networks, the proposed design enables dual linear polarization using only one feed and a minimal switching network, significantly reducing size and integration complexity. This paper introduces a novel single-port square patch antenna that achieves polarization reconfigurability. The proposed design is capable of switching between horizontal and vertical polarizations (HP and VP) respectively at approximately 5.35 GHz using a single RF excitation port. This innovative single-port approach simplifies the antenna's architecture, making it more compact than traditional multi-port designs. Such an antenna, with its ability to mitigate multipath fading, is especially well-suited for Wireless Local Area Networks (WLANs) operating in the mid-5G band (3.3–6 GHz).

II. ANTENNA DESIGN AND CONFIGURATION

A reconfigurable feeding geometry comprises of single excitation port and two microstrip lines are employed in this antenna. Desired linear polarization is achieved by selection of suitable RF current path with the help of ON state operation of corresponding PIN diode mounted on rectangular slots of the microstrip lines.

The evolution of the design can be understood as follows:

Step 1: Single-feed excitation along X-edge: A rectangular microstrip patch antenna is excited using a single microstrip feedline. The feedline is placed along the X-edge of the patch. This configuration excites the fundamental TM_{10} mode, resulting in horizontal linear polarization.

Step 2: Single-feed excitation along Y-edge: The feed is relocated along the orthogonal (Y-edge) of the patch. This excites the TM_{01} mode, producing vertical linear polarization. This step proves that polarization is governed by feed location.

Step 3: Integration of dual orthogonal feedlines: At last step both feedlines are incorporated simultaneously and connected to a single RF port using PIN diode switches. By activating one feedline at a time, the antenna dynamically switches between TM_{10} and TM_{01} modes. Thus, enabling polarization reconfigurability.

Fig. 1 illustrates the configuration of the proposed polarization-reconfigurable microstrip antenna, implemented on an FR4 substrate with dimensions of $(35 \times 35 \times 1.6) \text{ mm}^3$. The radiating element comprises a square patch with a side length of 12.5 mm. RF excitation is facilitated through two orthogonally placed microstrip feed lines, each having a width of 0.8 mm, connected to adjacent sides of the patch.

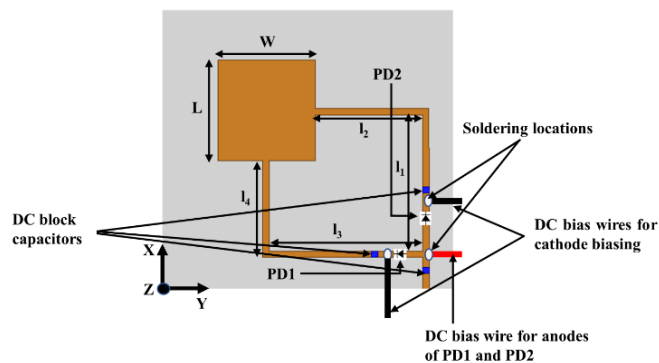


FIGURE 1. Top view of the designed antenna

These feed lines converge at a single RF input port via two PIN diode switches, designated as PD1 and PD2. To accommodate the integration of these PIN diodes, small rectangular slots are precisely etched onto the respective feed lines. The inclusion of the PIN diodes enables dynamic reconfiguration of the feed structure, thereby allowing selective excitation of only one patch edge at a time [18–19]. This controlled excitation mechanism enables the antenna to switch between two orthogonal linear polarizations—horizontal and vertical based on the biasing state of the PIN diodes.

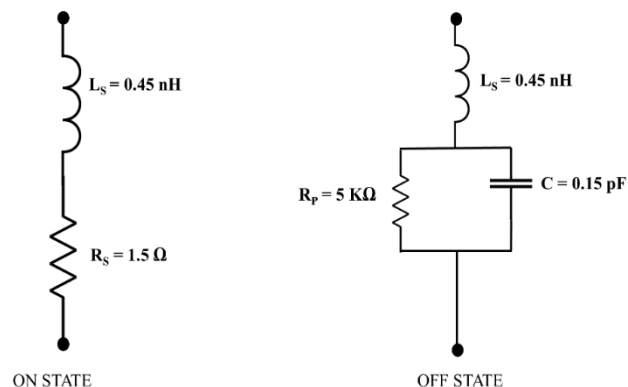


FIGURE 2. The equivalent circuit of the ON and OFF-state of the diode

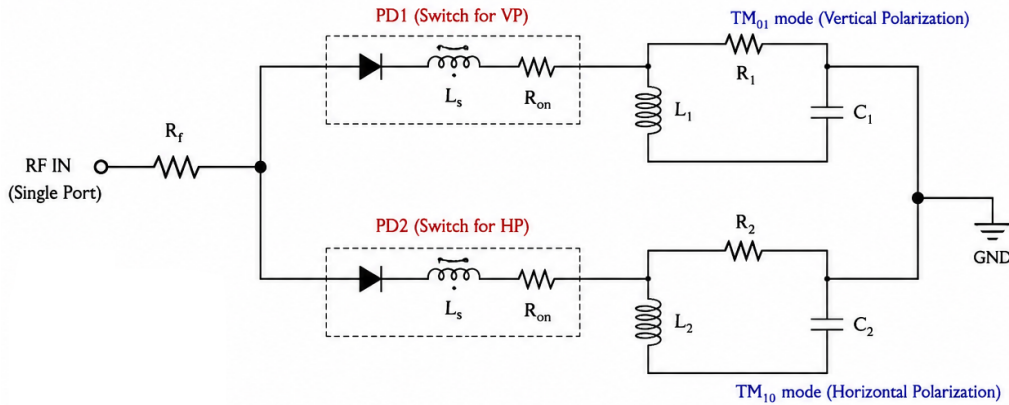


FIGURE 3. Equivalent circuit of the designed antenna

The equivalent circuit of the single-port polarization-reconfigurable patch antenna is shown in Fig.3. The RF signal from the single input port (RF) is fed through PIN diodes PD1 and PD2. These diodes are represented by their lumped-element parameters: series resistance (R_{on}) and inductance (L_s) in the ON-state, and a junction capacitance (C_{off}) in the OFF-state. The square patch is represented by two parallel RLC resonators. By suitably biasing the diodes, the signal is directed to either the L_1 - C_1 or L_2 - C_2 tank circuit, thereby exciting the respective orthogonal mode and achieving polarization reconfigurability.

A shared DC bias line providing a +3 V potential is soldered near the anodes of both PD1 and PD2. Additionally, two separate DC bias lines are soldered close to the cathodes of the respective diodes. In the diode's ON-state operation, the cathode bias line is left floating (i.e., no voltage is applied), whereas for the OFF-state, a forward bias of +5 V is applied to the cathode terminal, effectively rendering the diode non-conductive. The equivalent circuit of the ON and OFF-state of the diode is shown in Fig. 2.

To mitigate DC-RF interference and ensure signal integrity, three surface-mount device (SMD) capacitors with capacitance of 100 pF are strategically placed along the feed lines, as indicated in Fig. 1. These capacitors serve as DC blocks while allowing RF signal transmission.

The antenna structure and its various design parameters, including the positions of the feed points, the dimensions of the microstrip lines and the placement of the PIN diodes were optimized using Ansoft HFSS following transmission line model [16]. Notably, parametric analysis was deemed unnecessary for this design, as no individual design variable demonstrated a sufficiently significant impact on the antenna's performance to warrant such an investigation. The final optimized values of the key design parameters are enumerated in Table I.

TABLE I. OPTIMAL VALUES OF ANTENNA DESIGN PARAMETERS

SIDE LENGTH OF SQUARE PATCH	$L = W = 12.5$ MM
X-EDGE FEED LINE	$L_1 = 21.7$ MM, $L_2 = 13.9$ MM
Y-EDGE FEED LINE	$L_3 = 22.2$ MM, $L_4 = 13.4$ MM

III. POLARIZATION RECONFIGURATION: MODE ISOLATION

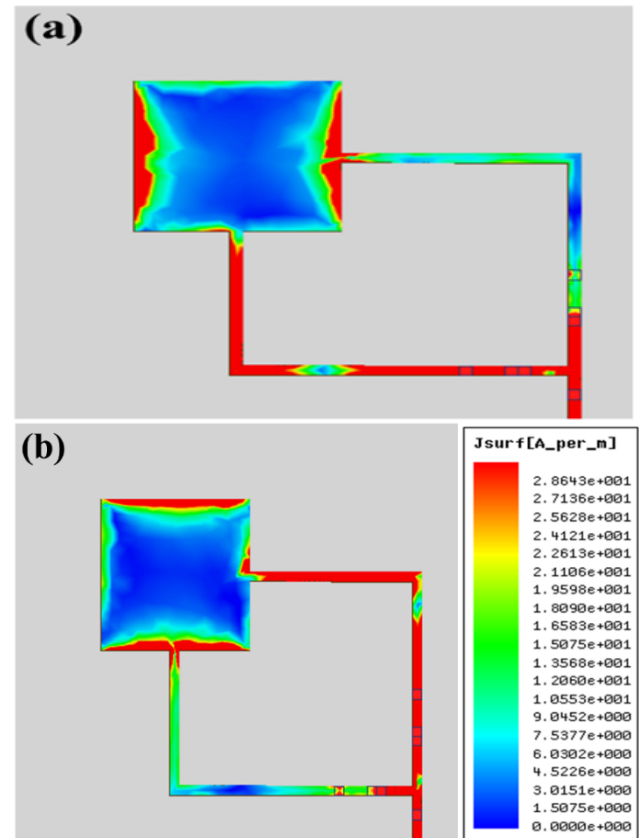


FIGURE 4. Surface current distribution (a) Mode 1, (b) Mode 2.

Reconfigurability in HP and VP linear polarization can be achieved by suitable selection of feed location in a microstrip patch antenna [20]. The proposed antenna uses two different feedlines to excite radiating patch at adjacent edges perpendicular to each other. ON state of the PIN diode associated with a specific feedline activates that RF current path. Switching one PIN diode at a time,

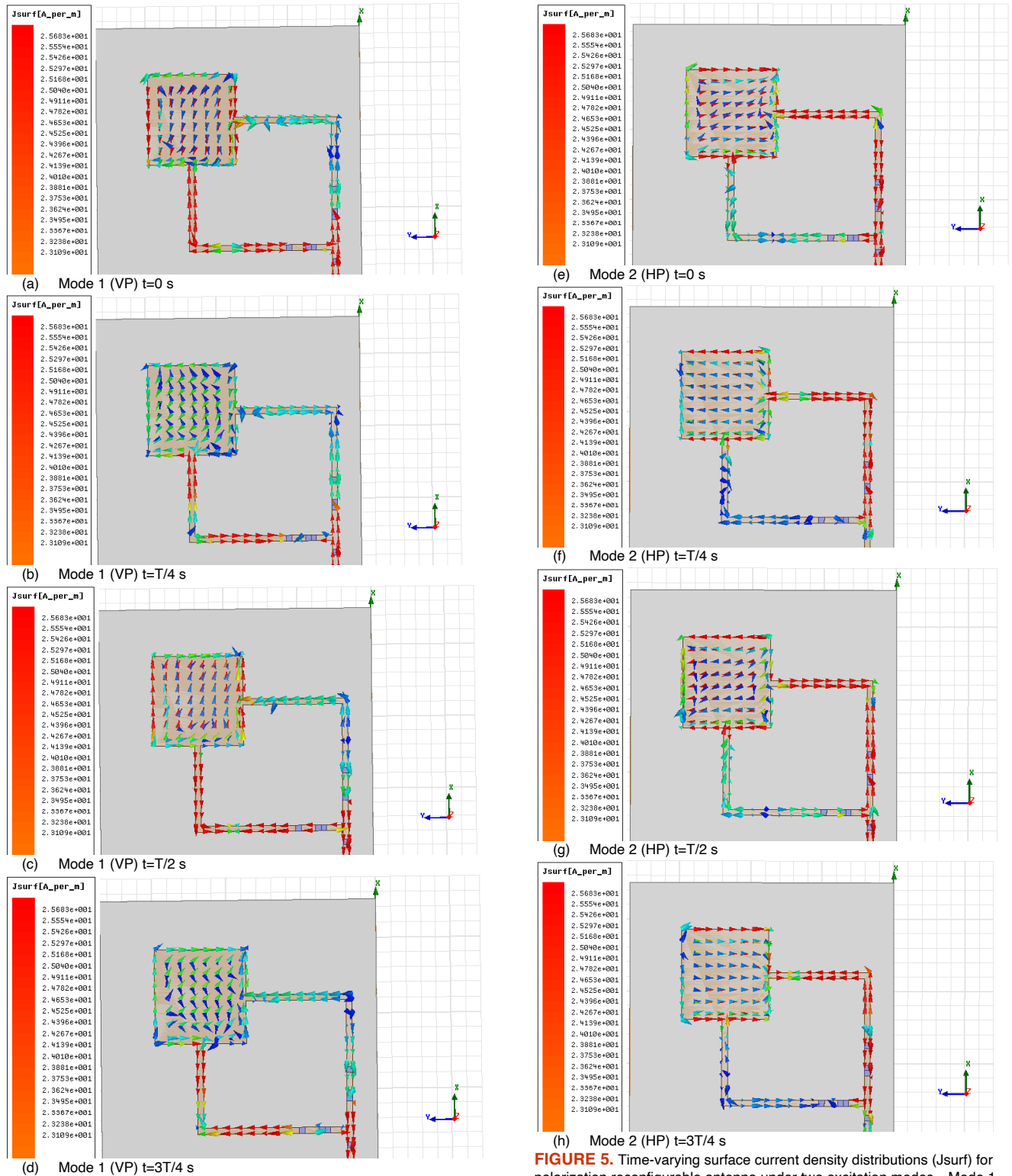


FIGURE 5. Time-varying surface current density distributions (J_{surf}) for polarization reconfigurable antenna under two excitation modes—Mode 1 (Vertical Polarization, VP) and Mode 2 (Horizontal Polarization, HP)—at four time phases of one RF cycle: $t=0, T/4, T/2, 3T/4$.

Polarization of the antenna can be switched between HP and VP. In the proposed antenna, when PD1 is turned ON, the antenna receives RF signal at Y-axis edge for excitation of TM_{01} mode and radiation edges are parallel to the Y-axis

to radiate VP wave (Mode 1 operation). Again, ON state operation of PD2 excites TM_{10} mode in the patch and radiation edges are parallel to the X-axis for HP (Mode 2 operation). Thus, switching of PD1 and PD2 produces linear polarization diversity in the proposed antenna. For validation of polarization reconfiguration mechanism, surface current distribution in mode 1 and 2 operations are shown in Fig. 4.

The time-varying surface current density distributions illustrated in the Fig. 5 provide critical insights into the polarization reconfigurability and modal behaviour [17] of the proposed microstrip patch antenna structure. The plots correspond to two distinct excitation modes—Mode 1 (Vertical Polarization, VP) and Mode 2 (Horizontal Polarization, HP), controlled by the ON-state of PIN diodes PD1 and PD2, respectively. Each mode is visualized at four key time instances: $t = 0, T/4, T/2$ and $3T/4$, capturing the evolution of current vectors over one RF cycle. The vector plots are superimposed with a color map representing current density magnitude (in A/m), offering both qualitative and quantitative validation of the modal field distribution.

A. MODE 1 – VERTICAL POLARIZATION (VP) WITH PD1 ON

Figs. 5(a) through 5(d) correspond to Mode 1, where the RF excitation is introduced via PD1, which activates the feedline along the Y-axis of the square patch. This configuration excites the TM_{01} mode, characterized by dominant current flow in the Y-direction, as evident from the orientation of the current vectors.

At $t=0$, Fig. 5(a), the surface current enters the patch from the active feedline and is symmetrically distributed along the vertical dimension of the patch. The opposing edges of the patch show clear current maxima, indicative of a standing wave pattern typical of the TM_{01} mode. The currents reverse direction at $t=T/2$ (Fig. 5c), maintaining the spatial symmetry and validating the sinusoidal nature of the excitation. Intermediate time steps, $t=T/4$ and $3T/4$ [Fig. 5(b) and 5(d)], show weakened or rotated vectors as the sinusoidal current reaches null crossing or phase reversal. The radiating edges parallel to the Y-axis dominate the radiation behaviour in this mode, thereby producing vertical linear polarization.

B. MODE 2 – HORIZONTAL POLARIZATION (HP) WITH PD2 ON

Figs. 5(e) to 5(h) depict the current distribution for Mode 2, with PD2 activated to introduce RF excitation along the X-axis edge of the patch. This excites the TM_{10} mode, in which the current is primarily oriented in the X-direction, as clearly observed from the vector fields. At $t = 0$ and $T/2$ [Fig. 5(e) and 5(g)], strong and unidirectional surface currents flow horizontally across the patch from the active feedline. This confirms excitation of TM_{10} , where the half-wavelength standing wave is aligned along the X-axis. As with the previous mode, the vectors reverse direction at half-cycle intervals, while intermediate time steps ($T/4$ and $3T/4$) show transitional vector states with rotational patterns

due to time-varying field reversal.

The radiation in this mode primarily originates from the patch edges parallel to the X-axis, confirming that the resulting electric field is oriented horizontally, hence achieving horizontal linear polarization. Importantly, there is negligible cross-polarized current component in both modes, reinforcing the high polarization purity of the antenna design.

A comparative analysis of Mode 1 and Mode 2 reveals that the antenna exhibits a clear modal orthogonality in both spatial and temporal domains. The orthogonal orientation of feedlines ensures that the excitation of TM_{01} and TM_{10} modes are spatially isolated, thereby offering high inter-port isolation. This behaviour directly contributes to the antenna's ability to support polarization diversity, which is essential for modern wireless systems, adaptive polarization matching or dual-polarized operation in harsh electromagnetic environments.

Furthermore, the magnitude of surface current density remains consistent across all four-time frames for each mode, confirming that the patch maintains impedance stability and mode confinement irrespective of the polarization state. The use of PIN diode switches introduces minimal disruption to the current flow paths due to careful placement and feeding structure design. As such, the proposed design successfully demonstrates dynamic polarization reconfigurability without compromising on modal integrity, gain performance or structural compactness.

IV. EXPERIMENTAL VALIDATION AND PERFORMANCE ANALYSIS

The single port antenna proposed for polarization diversity is fabricated as shown in Fig. 6. To validate the polarization reconfigurable operation of the proposed antenna, comprehensive measurements were conducted, with key results presented in Figs. 8 and 9 and Tables II and III.

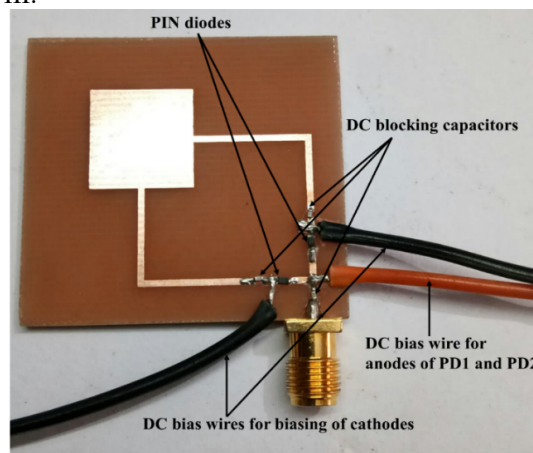


FIGURE 6. Photograph of the fabricated antenna.

As discussed in Section III, the antenna operates in two distinct polarization modes—Mode 1 (VP) and Mode 2 (HP)—controlled by selectively biasing the PIN diodes PD1 and PD2, respectively. The reflection coefficient S_{11} was measured for both modes using a calibrated vector

network analyser [Fig. 7(a)]. For Mode 1, with PD1 turned ON to excite the TM_{01} mode (vertical polarization), the simulated resonant frequency is 5.31 GHz, while the measured resonance occurs at 5.40 GHz. Similarly, for Mode 2, where PD2 is ON to activate the TM_{10} mode (horizontal polarization), the simulated and measured resonant frequencies are 5.27 GHz and 5.33 GHz, respectively. The slight shifts observed between simulation and measurement are attributed to fabrication tolerances, soldering imperfections, substrate dielectric variation and the presence of DC bias lines which introduce minor parasitic effects not accounted for in ideal simulations.

The measured S_{11} plots (Fig. 8) closely follow the simulated trends in both modes. Specifically, Mode 1 exhibits a minimum S_{11} of -13.1 dB at 5.40 GHz, while Mode 2 demonstrates a deeper reflection dip at -18.3 dB near 5.33 GHz. The measured -10 dB impedance bandwidths are 3.52% and 6.01% for Modes 1 and 2, respectively, showing profound agreement with the simulated bandwidths (3.58% and 6.83%) as listed in Table II. This confirms that the antenna maintains effective impedance matching and polarization integrity across its operating frequency range in both modes.

Further, the radiation characteristics of the fabricated antenna were measured in an anechoic chamber [Fig. 7(b)] to assess the beam profile and polarization behavior.

The E- and H- plane radiation patterns for both VP and HP modes are depicted in Figs. 9(a) and 9(b), respectively. The measured patterns closely align with their simulated counterparts, demonstrating symmetric main lobes and low back lobe radiation—characteristics desirable for directive and polarization-stable antennas. Minor asymmetries observed in the measured patterns are likely due to the influence of connector orientation, feed cable bending and minor geometric deviations in the fabricated prototype.

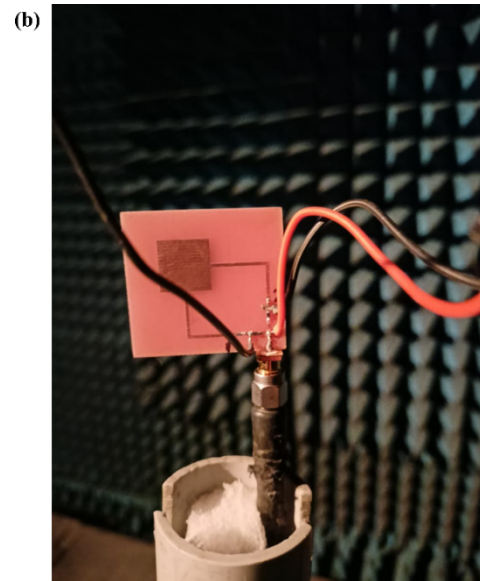


FIGURE 7. Measurement of the fabricated antenna in (a) VNA, (b) Anechoic chamber.

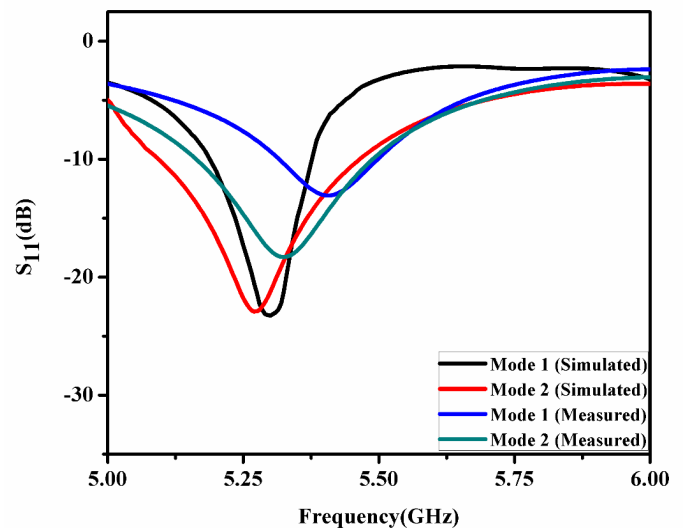


Figure 8. Comparative S_{11} plot for mode 1 and mode 2 operation

TABLE II. Comparison of simulated and measured s_{11} parameters (sim=simulated and msd=measured)

Modes of operation	Resonant frequency (GHz)		Reflection coefficient S_{11} (dB)		-10 dB % bandwidth	
	Sim.	Msd.	Sim.	Msd.	Sim.	Msd.
Mode 1	5.31	5.40	-23.1	-13.1	3.58	3.52
Mode 2	5.27	5.33	-22.9	-18.3	6.83	6.01

TABLE III. Comparative results of AR and gain

Modes	Axial ratio (dB)		Gain (dBi)		Simulated antenna efficiency (%)
	Sim.	Meas.	Sim.	Meas.	
Mode 1	52	48	2.81	2.48	74
Mode 2	55	51	2.95	2.76	81

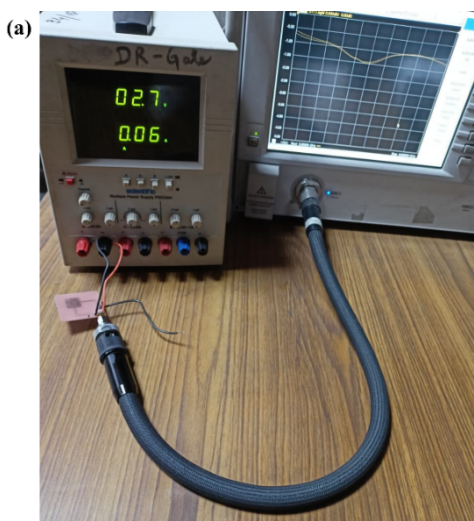


TABLE IV. A comparison of the proposed antenna with recent published work:

Reference	Size (mm ²)	Bandwidth (%)	Technique	Peak Gain (dBi)	Polarization Type	Applications
[2]	Compact	UWB / Notched UWB	PIN Diode-Enabled	-2.1	---	UWB Communication
[3]	Not Specified	Not Specified	Advanced Materials	Not Specified	---	Advanced Engineering
[4]	Flexible	Tri-band	Multi-stub loaded / PDMS	Not Specified	---	Heterogeneous / Wearable
[21]	45 x 45	4.1	Dual Port	2.5	Circular	Satellite
[22]	38 x 38	5.2	Varactor diode	2.3	Frequency	WLAN
Proposed Work	35 x 35	3.52 (VP) / 6.01 (HP)	PIN Diode (Single-Port switching)	2.76	Linear (HP/VP)	Mid-band 5G (3.3–6 GHz)

To further affirm the linear polarization quality, the axial ratio (AR) was computed and measured. The AR values for Mode 1 and Mode 2 are found to be 48 dB and 51 dB, respectively, as shown in Table III, which confirm excellent linear polarization performance with negligible circular or cross-polarized components. The gain measurements yielded peak values of 2.48 dBi (Mode 1) and 2.76 dBi (Mode 2), slightly lower than the simulated values of 2.81 dBi and 2.95 dBi, respectively. The reduction can be attributed to practical losses in the substrate, solder joints and finite ground effects.

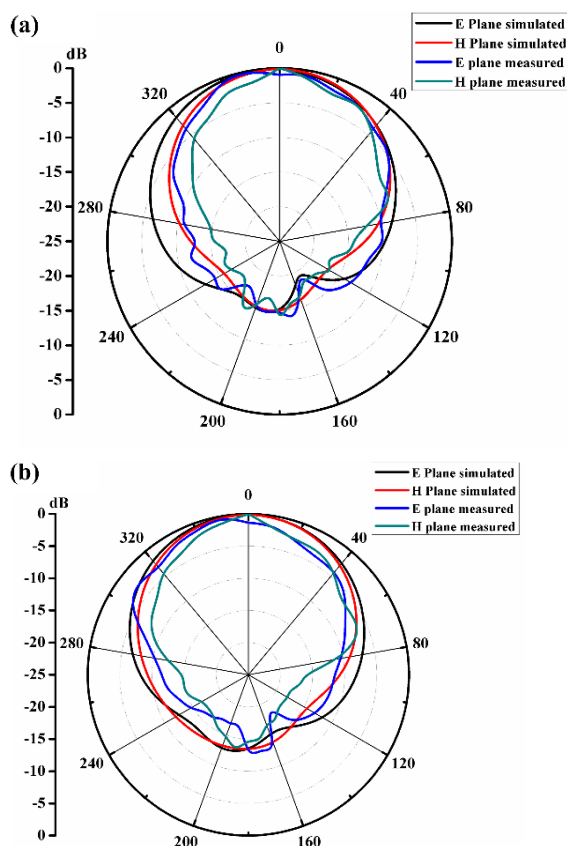


Figure 9. Comparative radiation pattern plots of (a) Mode 1, (b) Mode 2 operation.

A comparison table of the current work with other works is presented in Table IV, it is evident that, the novelty of the

work lies in the single-port approach to achieve dual linear polarization (Vertical and Horizontal). While most Polarization Reconfigurable Antennas (PRAs) rely on multiple ports, which increases the antenna footprint and necessitates additional RF circuitry. This design achieves high modal isolation and polarization agility using a simplified, orthogonally placed feedline structure integrated with PIN diodes. This makes it well-suited for miniaturized mid-band 5G applications where spectral efficiency and link reliability are critical.

V. CONCLUSION

A reconfigurable feed geometry-based single-port microstrip patch antenna with dynamic linear polarization diversity has been successfully developed and validated in this work. The proposed design enables polarization switching between vertical and horizontal modes by selectively biasing PIN diodes mounted on orthogonally placed microstrip feedlines, all connected to a single RF excitation port. This compact and planar configuration introduces significant advantages in terms of simplicity, integration and adaptability for modern wireless systems. The fabricated prototype was rigorously evaluated for key performance parameters, including reflection coefficient (S_{11}), radiation pattern, gain, and axial ratio. The antenna achieves -10 dB impedance bandwidths of 3.52% (VP) and 6.01% (HP), peak gains of 2.48 dBi and 2.76 dBi and axial ratios above 48 dB, confirming high polarization purity and low cross-polarization. The measured results demonstrate strong agreement with simulation, confirming the reliability of the design methodology. Resonant frequencies for both polarization modes are observed around 5.35 GHz, with stable broadside radiation patterns and an average gain of approximately 2.62 dBi across modes. The antenna also exhibits excellent polarization purity, validating its suitability for applications requiring reconfigurable polarization. The antenna architecture is particularly relevant for mid-band 5G communication systems, where polarization agility is critical performance requirements.

REFERENCES

- [1] L. Malviya, J. Malik, R. K. Panigrahi and M. V. Kartikeyan, "Design of a compact MIMO antenna with polarization diversity technique for wireless communication", 2015 International Conference on Microwave, Optical and Communication Engineering (ICMOCE), Bhubaneswar, India, pp. 21-24(2015).

- [2] M. Hussain, W.A. Awan, A. Alwabri, *et al.*, “A PIN diode-enabled compact size antenna for transition between UWB and notched UWB modes,” *Arab. J. Sci. Eng.* **50**, 17759–17768 (2025).
- [3] M. Hussain, W.A. Awan, S.M. Abbas, Y. Zhu, “Advanced engineering materials-based antenna design,” *Adv. Eng. Mater.* **27**, e202502127 (2025). <https://doi.org/10.1002/adem.202502127>
- [4] M. Hussain, S.M. Abbas, Y. Zhu, “Multi-stub loaded tri-band flexible antenna based on PDMS for heterogeneous applications,” in *Proc. URSI Asia-Pacific Radio Science Meeting (AP-RASC)* (IEEE, 2025).
- [5] T. Itoh, G. Haddad, and J. Harvey, *RF Technologies for Low Power Wireless Communications*. New York: Wiley(2001).
- [6] S. Gao, A. Sambell, and S. S. Zhong, “Polarization-agile antennas”, *IEEE Antennas Propagation Magazine*, Vol. 48, No. 3, pp. 28–37(2006).
- [7] Y. J. Sung, “Reconfigurable patch antenna for polarization diversity”, *IEEE Transaction Antennas Propagation*, Vol. 56, No. 9, pp. 3053–3054(2008).
- [8] Khaleghi and M. Kamyab, “Reconfigurable single port antenna with circular polarization diversity”, *IEEE Transaction Antennas Propagation*, Vol. 57, No. 2, pp. 555–559, Feb. 2009.
- [9] Y. Sung, “Investigation into the polarization of asymmetrical feed triangular microstrip antennas and its application to reconfigurable antennas”, *IEEE Transaction Antennas Propagation*, Vol. 58, No. 4, pp. 1039–1046(2010).
- [10] F. Yang and Y. Rahmat-Samii, “A reconfigurable patch antenna using switchable slots for circular polarization diversity”, *IEEE Microwave Wireless Components Letters*, Vol. 12, No. 3, pp. 96–98(2002).
- [11] Y. J. Kim, J. K. Kim, J. H. Kim, and H. M. Lee, “Reconfigurable annular ring slot antenna with circular polarization diversity,” in *Proceedings of Asia-Pacific Microwave Conference*, pp. 1–4(2007).
- [12] W. M. Dorsey, A. I. Zaghloul, and M. G. Parent, “Perturbed square-ring slot antenna with reconfigurable polarization”, *IEEE Antennas and Wireless Propagation Letters*, Vol. 8, pp. 603–606(2009).
- [13] J. S. Row and C. J. Shih, “Polarization-diversity ring slot antenna with frequency agility”, *IEEE Transaction Antennas Propagation*, Vol. 60, No. 8, pp. 3953–3957(2012).
- [14] J. S. Row, W. L. Liu, and T. R. Chen, “Circular polarization and polarization reconfigurable designs for annular slot antennas,” *IEEE Trans. Antennas Propag.*, Vol. 60, No. 12, pp. 5998–6002(2012).
- [15] Y. Cao, S. W. Cheung, and T. I. Yuk, “A Simple Planar Polarization Reconfigurable Monopole Antenna for GNSS/PCS,” *IEEE Transaction Antennas Propagation*, Vol. 63, No. 2, pp. 500–507(2015).
- [16] A. Bharathi, M. Lakshminarayana, P.V.D.S. Rao, “A Quad-Polarization and Frequency Reconfigurable Square Ring Slot Loaded Microstrip Patch Antenna for WLAN Applications”, *AEU - International Journal of Electronics and Communications*, Vol.78, pp. 15-23(2017).
- [17] F. Antunes, A. Ramos, T. Varum and J. N. Matos, “Concept and Design of a Multi-Polarization Reconfigurable Microstrip Antenna with Symmetrical Biasing Control”, *Sensors*, Vol. 24, No. 8, 2408, pp. 1-14(2024).
- [18] A. Chowdhury and P. Ranjan, “A novel PIN diode-based frequency reconfigurable patch antenna with switching between the mid-5G and high-5G frequency band”, *International Journal of Microwave and Wireless Technologies*, Vol. 16, No. 4, pp. 595-604(2024).
- [19] A. K. Abd, J. M. Rasool, Z. -A. S. A. Rahman, Y. I. A. Al-Yasir, “Design and Analysis of Novel Reconfigurable Monopole Antenna Using Dip Switch and Covering 5G-Sub-6-GHz and C-Band Applications”, *Electronics* 2022, Vol. 11, 3368, pp. 1-18(2022).
- [20] R. Garg, P. Bhartia, I. Bahl and A. Ittipiboon, “Handbook of microstrip antenna”, Artech House, (2001).
- [21] Y. Li, *et al.*, “Polarization-reconfigurable antenna using combination of circular polarized modes,” *IEEE Access* **9**, 43852–43860 (2021).
- [22] S. Kumar, *et al.*, “Reconfigurable antenna with varactor diodes for wireless systems,” *Alex. Eng. J.* **68**, 123–131 (2023).